# ANALYSIS OF THE TECHNICAL VIABILITY OF GFRP REINFORCED PRECAST CONCRETE PILES

J. D. Jimenez Vicaria[a], D. Fernandez Diaz[a], E. Manzano Arroyo[b], C. Paulotto[a*]

[a]*ACCIONA Infraestructuras, S.A., Alcobendas (Spain)*
[b]*Terratest, S.A., Madrid (Spain)*
[*]*carlo.paulotto@acciona.com*

**Keywords:** GFRP, pile, driving, testing

**Abstract**
*The use of glass fiber reinforced polymer (GFRP) bars, as reinforcement for concrete structures, has been developed in the last decades to address the durability issue raised by the corrosion of steel reinforcement. However, it is not possible to replace directly steel bars for GFRP ones due to the differences between the mechanical properties of these two materials. In particular, the behavior of GFRP bars used as longitudinal reinforcement in concrete elements subjected to compression loads, such as reinforced concrete piles, is still to be clarified. In this paper the results of a series of experimental tests carried out on full-scale prototypes of precast concrete piles reinforced with GFRP bars are presented. The conclusions derived from the comparison between the results of high-strain dynamic tests performed on driven piles reinforced with GFRP and steel bars are discussed.*

## 1. Introduction

When concrete structures are located in harsh environment, to provide extra corrosion protection to black carbon steel reinforcing bars, concrete cover is normally increased. Unfortunately, in the case of precast steel reinforced concrete piles, concrete cover should not be increased further than approximately 35 mm since a thicker cover would be extremely prone to spall during the pile driving. In this case, the use of GFRP reinforcing bars may improve the durability of concrete piles without increasing the concrete cover. To analyze this solution, a set of precast concrete piles reinforced with GFRP bars was designed to have the same axial and lateral bearing capacity of a standard pile reinforced with steel bars. GFRP reinforced concrete piles were manufactured, driven and tested to assess the technical viability of this technology.

## 2. Experimental program

### *2.1. Design and manufacture of the test specimens*

The transversal cross-sections of the steel and GFRP reinforced piles analyzed in the present research work are shown in Figure 1, while the mechanical properties of the basic materials employed in their design are summarized in Table 1. The interaction diagrams corresponding to the cross-sections shown in Figure 1 are plotted in Figure 2. To obtain the axial-bending interaction diagram and the axial-shear interaction diagram of the GFRP reinforced piles, the requirements of *Article 42* and *Article 44* of the EHE-08 [1] were implemented in a

spreadsheet, taking into account the particular characteristics of the GFRP reinforcement in accordance with the existing design recommendations [2], [3], [4].

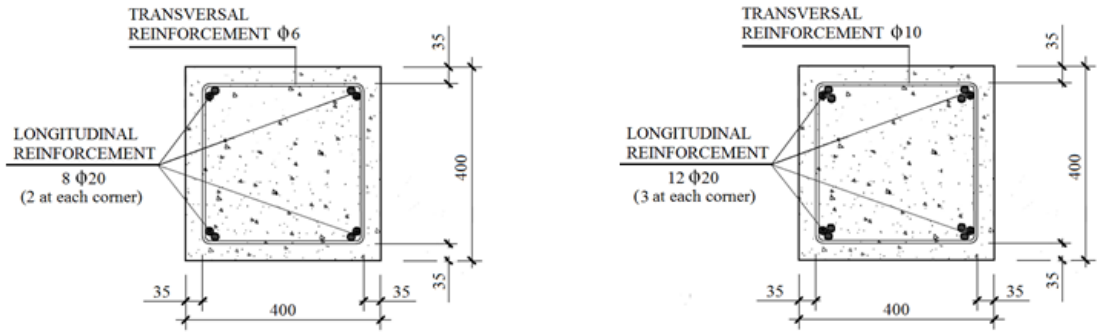


a) b)

**Figure 1.** a) Cross-section of the piles reinforced with steel bars and b) cross-section of the GFRP reinforced piles (dimensions in mm).

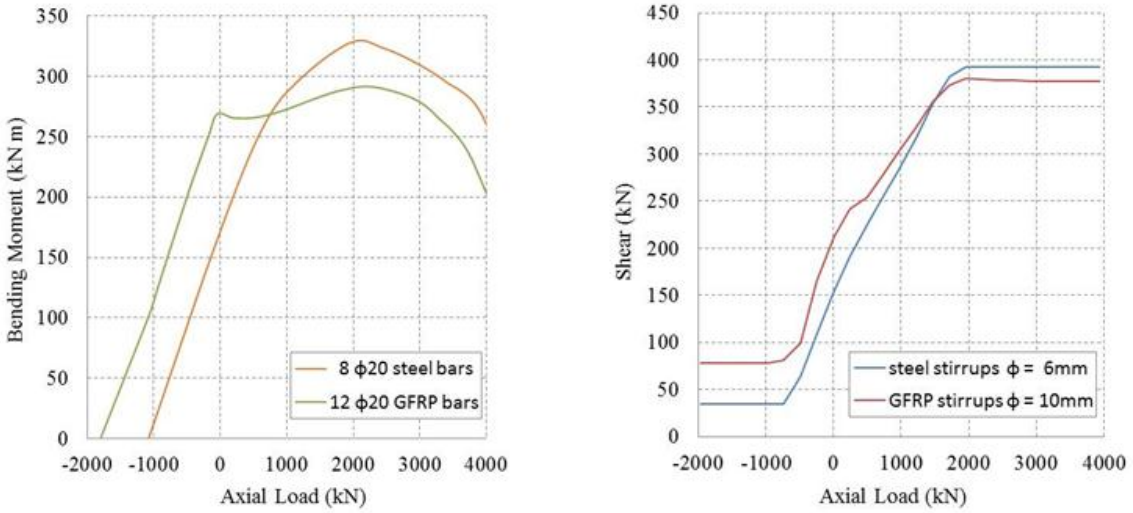


a) b)

**Figure 2.** a) Axial load - bending moment interaction diagrams for steel and GFRP reinforced piles; b) Axial load - shear interaction diagrams for steel and GFRP reinforced piles.

| ***Concrete HA-50*** | ***Steel B500SD*** | ***GFRP reinforcement*** |
|---|---|---|
| $E_c$ = 33 GPa | $E_s$ = 200 GPa | $E_f$ = 40.8 GPa |
| $f_{ck}$ = 50 MPa | $f_{yk}$ = 500 MPa | ϕ 20 $f_{fk}$ = 620 MPa |
| | | ϕ 10 $f_{fk}$ = 760 MPa (straight portion) |
| | | ϕ 10 $f_{fk}$ = 292 MPa (bent portion) |

**Table 1.** Mechanical properties of the basic materials employed in the pile design.

A total of eight GFRP reinforced piles were manufactured (Figure 3a). The present paper describes the results obtained from the analysis of the driving process of piles P5, P6, P7 and P8 (Figure 3b). These four piles were all monolithic with a length of 12 m. Piles P5 and P6 were longitudinally and transversally reinforced with GFRP bars, while piles P7 and P8 were steel reinforced.


**Figure 3.** a) GFRP piles reinforcement cages; b) Pile P5 during its driving.

Mechanical tests were carried out on the basic materials employed to manufacture the GFRP reinforced piles. Three concrete cylindrical specimens were prepared and cured in the same outdoor condition of the piles. They were tested in compression according to the UNE-EN 12390 during the week in which piles were driven, at an age of 56 days. An average value of 47.7 MPa was obtained. Tensile tests were performed on two 20 mm diameter GFRP bars belonging to the same batch of the bars used to reinforce the piles. The tests were performed according to ACI 440.3R-04 [5]. An average value of 43.8 GPa and 926 MPa was obtained for the elastic modulus and the tensile strength, respectively.

*2.2. Geological characteristics of the soil at the testing site*

All the piles were driven in the soil at the same site in the proximity of the village of Benacazon in the South of Spain. This village is at the edge of the depression of the Guadalquivir River, which is formed by horizontal layers of marine and fluvial deposits. From the results of a probing well drilled in the proximity of the testing site, it can be deduced that, till a depth of approximately 30 m, the subsoil is formed by sand and clay, while the water tab is at a depth of approximately 5 m from the ground level [6].

*2.3. Test procedure and results*

During the handling of the piles, due to their own weight, cracks appeared in the concrete at the tensioned faces of the piles. In the case of GFRP reinforced piles, these cracks appeared to be wider and more developed than those induced in the steel reinforced piles (Figure 4). An average crack width of 0.30 mm and 0.10 mm was measured for the GFRP and steel reinforced piles, respectively. This difference is mainly due to the lower axial stiffness of the GFRP reinforcement respect to that of steel reinforcement.

The four piles, from P5 to P8, were driven using a piling hammer with a 9 t ram and a constant drop height of 0.40 m till reaching practical refusal. The blow counts per 0.20 m of penetration are diagrammed in Figure 5 for the four piles. The pile driving was also monitored using the Case Method [7] (Figure 6). With this aim, an accelerometer and an extensometer were attached to opposite sides of the piles and connected to a Pile Driving Analyzer® (PDA). After the driving process, a dynamic load test was also performed on each pile to obtain its geotechnical capacity load according to ASTM D4945-12 [8]. During the dynamic load tests the drop height was increased to 1.20 m. Figure 7 shows the time-histories, in term of force

and velocity, recorded by the sensors applied to the piles during one blow of the dynamic test they were submitted to. The results of the dynamic tests are summarized in Table 2.

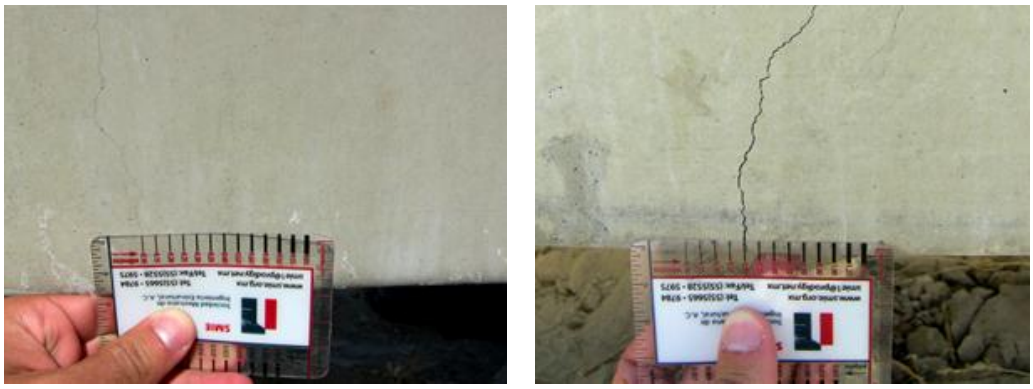

a) b)

**Figure 4.** Cracking in the tensioned face of the stored piles due to their own weight: a) a steel reinforced pile; b) a GFRP reinforced pile.

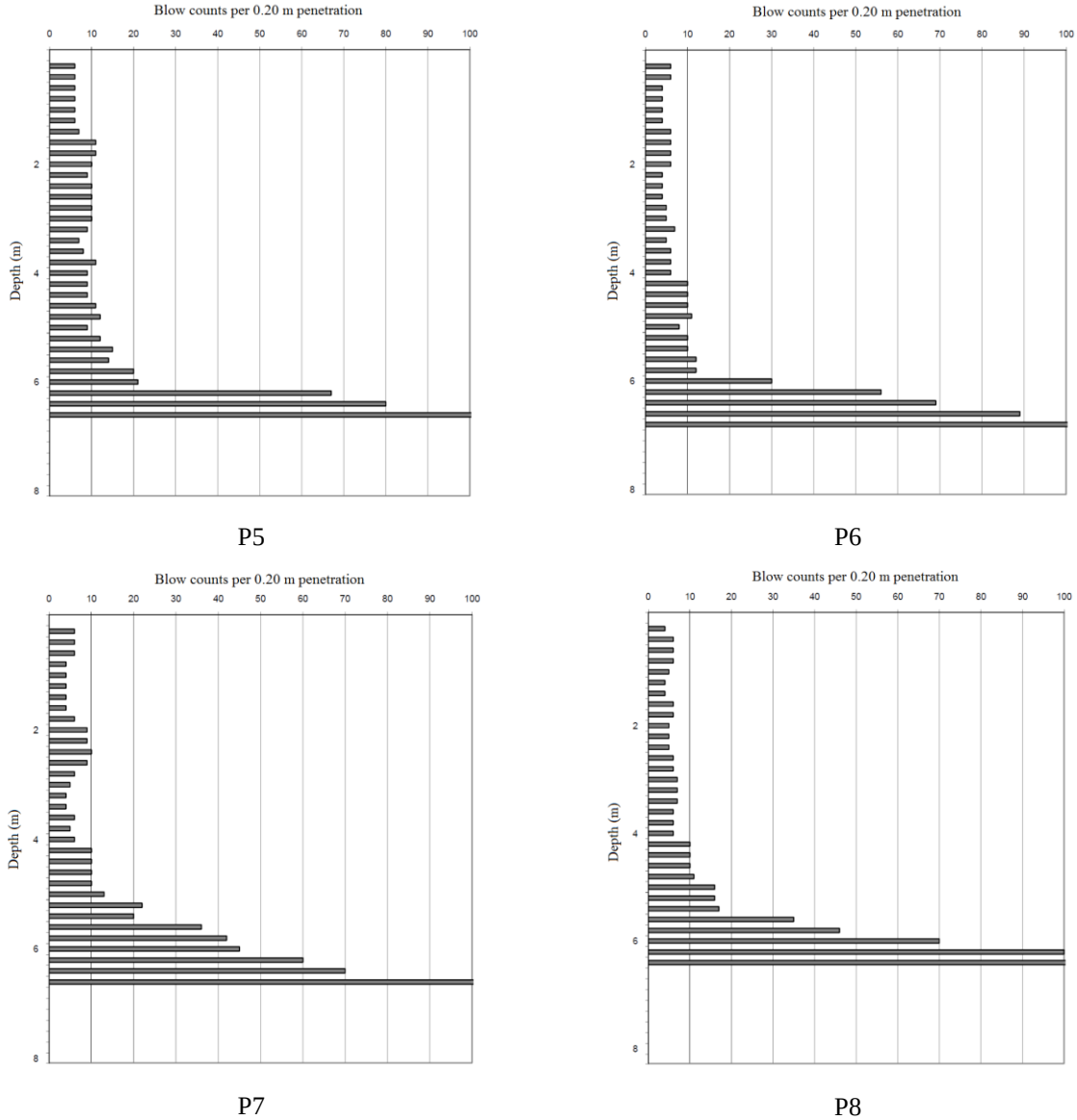


**Figure 5.** Blow counts per 0.20 m of penetration during pile driving.

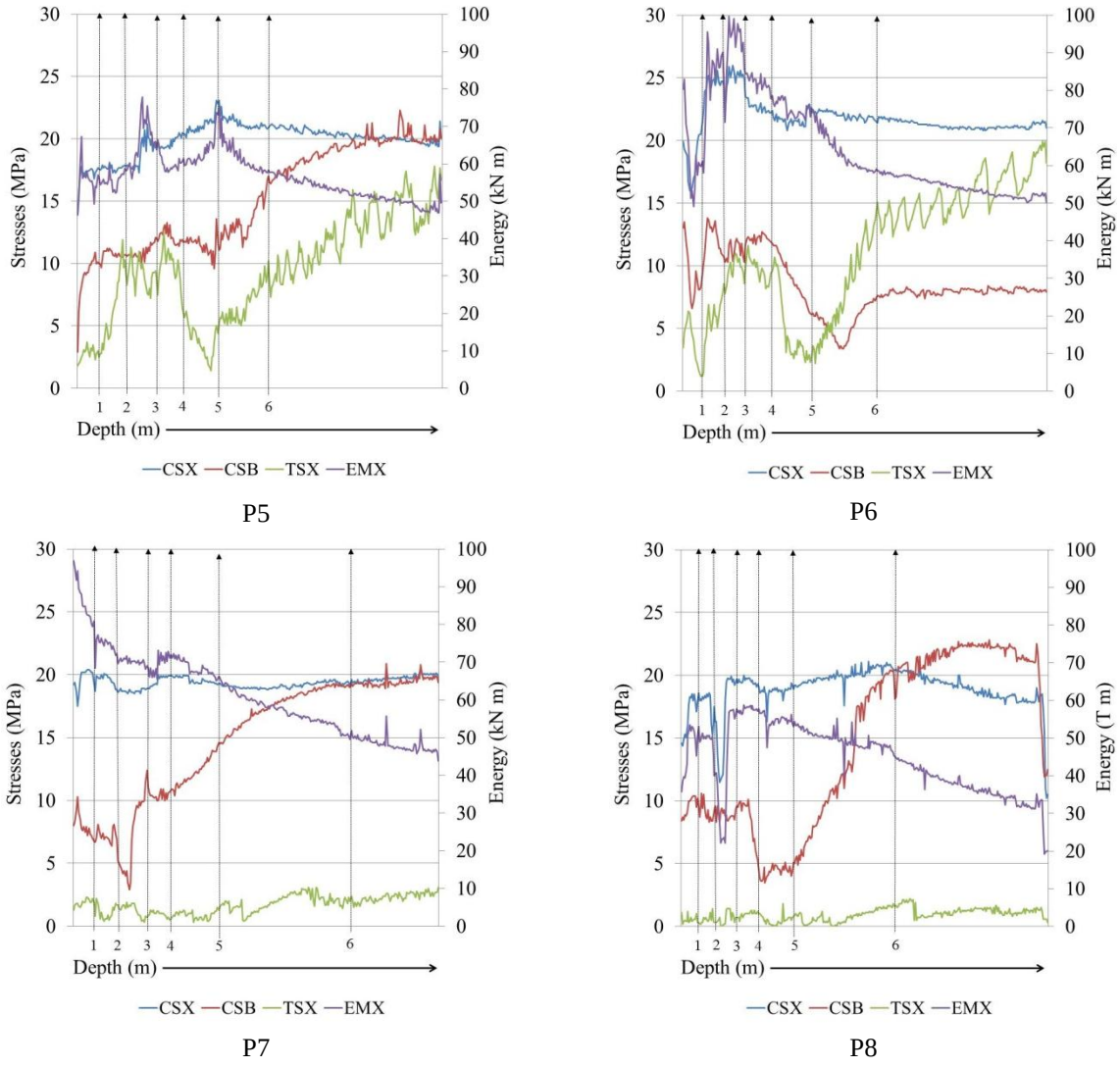


**Figure 6.** Stresses and energy measured during piles installation (CSX: top compression stress; CSB: toe compression stress; TSX: top tensile stress; EMX: maximum energy transmitted to the pile).

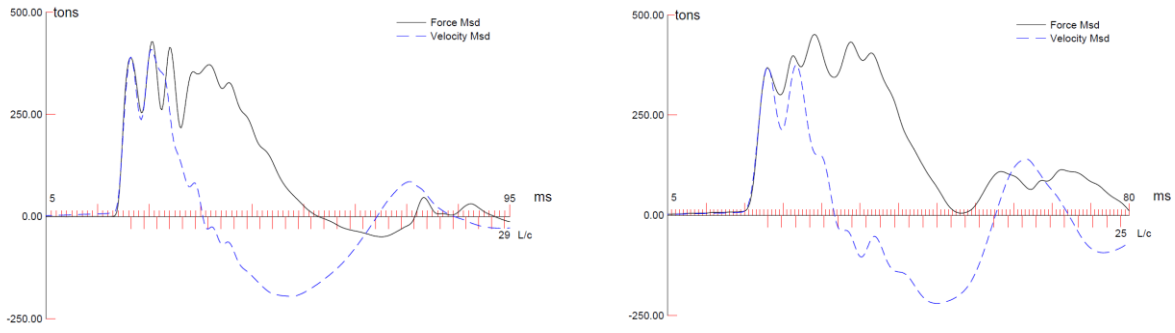

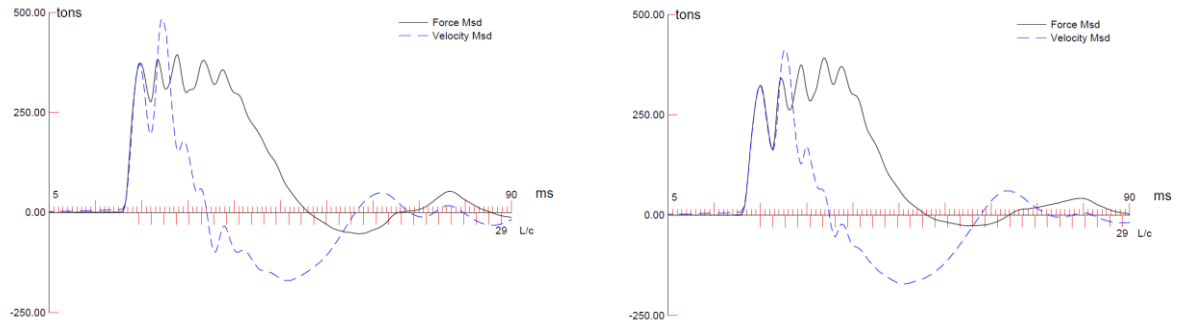


**Figure 7.** Measured force and velocity recorded during one blow of the dynamic test.

| Pile designation | | Driven Length (m) | Mobilized Resistance (kN) | | |
|---|---|---|---|---|---|
| | | | Along shaft | At toe | Total |
| P5 | GFRP | 6.60 | 1068 | 2969 | 4037 |
| P6 | GFRP | 6.80 | 1225 | 3499 | 4724 |
| P7 | STEEL | 6.60 | 1196 | 3038 | 4234 |
| P8 | STEEL | 6.40 | 853 | 3116 | 3969 |

**Table 2.** CAPWAP-W analysis results for the driven piles.

### *2.4. Analysis of the results*

The mechanical behavior of the piles was monitored during their driving using the Case Method. This method is based on the one-dimensional propagation theory for mechanical waves. According to this theory, for a uniform elastic rod impacted at one end, proportionality exists between force and velocity as long as no waves travel in the opposite direction [9]. Thus, for a uniform pile of length $L$ with no soil resistance, the measured pile top force, $F$, and velocity, $v$, are related by $F = (EA/c)v$ until time $2L/c$ after the impact. The quantity $EA/c$ is known as the pile impedance, where $E$ is the elastic modulus of the pile material, $A$ the cross-section of the pile, and $c$ the stress wave speed. The amount of separation, $F – (EA/c)v$, at any time $t$, after impact, is usually caused by the sum of soil resistance acting above a distance $x = ct/2$ below the pile top. Other contributions to this separation are given by changes in cross-section. If a pile changes its cross-section at a depth $x$, then at the time $2x/c$ after impact, a wave effect can be observed at the pile top in both force and velocity records [10]. An increase in pile cross-sectional area causes the pile top force to increase relative to the velocity. A cross-sectional reduction, such as that due to mechanical damage of the pile, causes the opposite effect. The Case Method can then be used to determine the driving induced pile damage [11].

From qualitative inspections of the curves shown in Figure 7, it can be observed that for all the piles the first reflection happens at approximately $L/c$ from the ram impact. This is due to a discontinuity located approximately at 2 m below the ground level and probably corresponding to the passage from the superficial layer of organic soil to the underlying layer formed by sand and clay. It can also be noted that the force and velocity traces corresponding to piles P6 and P7 separates at $L/c$, with the force trace going above the velocity one. This can be explained by a transition from a softer to a stiffer soil layer. This observation is supported by the graphs shown in Figure 5 that indicate a higher number of blows at this level.

The second reflection happens at *2L/c* for all the piles. At this instant, the velocity traces are at the same level or above the force traces but a short time after that, the velocity goes negative and the force increases showing a strong, but delayed tip resistance. This is typical of large soil quakes [12]. In practicality, this is generally referred to as 'bouncy driving'. This is an unfavorable condition because it renders the driving process inefficient and allows the development of possibly damaging tensile stress in concrete piles. Compressive and tensile stresses during the pile driving are shown in Figure 6. It is apparent that the tensile stresses in the GFRP reinforced piles are higher than those induced in the steel reinforced ones, probably due to the lower tensile axial stiffness of the GFRP reinforced piles, which exhibit greater crack opening during the pile driving. During the high-strain dynamic tests carried out after the pile driving and which results are shown in Figure 7 no sign of damage was detected for any of the piles. The maximum registered compressive stress were around 32 MPa for all the piles and higher than those experimented during the driving, while the maximum tensile stresses for the GFRP reinforced piles were sensibly lower (4.57 MPa for pile P5 and 1.31 MPa for pile P6) respect to those experimented during the pile driving. During the high-strain dynamic tests the drop height of the ram was increased to 1.20 m.

## 3. Conclusions

The following conclusions can be drawn from the analysis of the results:

1. Due to the tension stresses induced in the piles during their handling, the GFRP reinforced piles exhibit wider cracks respect to the equivalent steel reinforced piles. This does not represent an issue for the durability of the piles reinforced with GFRP bars since those do not suffer from galvanic corrosion. Nevertheless, this might represent an aesthetic problem that can affect the client-side acceptance.

2. The pile driving was very demanding for the structural integrity of the piles due to the particular soil conditions at the testing site. Large tensile stresses (> 15 MPa) were developed in the GFRP piles. Nevertheless, no sign of damage was detected in these piles during the high-strain dynamic tests carried out after the driving.

3. The positive results of the tests described in the present paper seem to suggest the technical viability of the use of precast GFRP reinforced concrete piles in harsh environments and the possibility of installing them following the procedure normally employed for precast concrete piles reinforced with steel bars.

## References

[1] *EHE-08. Instrucción de Hormigón Estructural*. Ministerio de Fomento. Gobierno de España.

[2] *fib Bulletin 40. FRP reinforcement in RC structures*. fib-The International Federation for Structural Concrete, Lausanne, Switzerland, 2007.

[3] *CNR-DT 206/2006. Guide for the Design and Construction of Concrete Structures Reinforced with Fiber-Reinforced Polymer Bars*. National Research Council, Rome, Italy, 2006.

[4] *ACI 440.1R-06. Guide for the Design and Construction of Structural Concrete Reinforced with FRP Bars*. American Concrete Institute, Committee 440, Farmington Hills, MI, USA, 2006.

[5] ACI 440.3R-04: *Guide Test Methods for Fiber-Reinforced Polymers (FRPs) for Reinforcing or Strengthening Concrete Structures*. American Concrete Institute, Farmington Hills, MI, 2004.

[6] *Actividad 2: Apoyo a la caracterización adicional de las masas de agua subterránea en riesgo de no cumplir los objetivos medioambientales en 2015. Demarcación Hidrográfica del Guadalquivir. MASA DE AGUA SUBTERRÁNEA 050.050 Aljarafe*. Ministerio de Ciencia e Innovación, y Ministerio de Medio Ambiente y Medio rural y Marino. Gobierno de España.

[7] G. G. Goble, F. Rausche, and G. Likins. Bearing Capacity of Piles from Dynamic Measurements, *Final Report*. *Report No. OHIO-DOT-05-75*, Ohio Department of Transportation, Department of Solid Mechanics, Structures and Mechanical Design, Case Western Reserve University, March, 1975.

[8] ASTM D4945-12. *Standard Test Method for High-Strain Dynamic Testing of Deep Foundations*.

[9] M. Hussein and G. G. Goble. Qualitative Evaluation of Force and Velocity Measurements During Pile Driving. *Dynamic Response of Pile Foundations*, Reston, VA, 166-183, April 1987.

[10] F. Rousche and G.G. Goble. Determination of Pile Damage by Top Measurements. American Society for Testing and Materials. *Special Publication, American Society for Testing and Materials*. Philadelphia, PA, 500-506, 1979.

[11] S. Webster and W. Teferra. Pile Damage Assessments using the Pile Driving Analyzer. *Proceeding of the 5th International Conference on the Application of Stress-wave Theory to Piles*, Orlando, FL, 759-772, September 1996.

[12] G. E. Linkins. Pile Installation difficulties in Soils with Large Quakes. *Dynamic Measurement of Piles and Piers*, American Society of Civil Engineers, Geotechnical Engineering Division, Philadelphia, PA, May 1983.